Meteoritics & Planetary Science 40, Nr 4, 529–540 (2005)
Abstract available online at http://meteoritics.org

Matching Martian crustal magnetization and magnetic properties of Martian meteorites

Pierre ROCHETTE[1*], Jérôme GATTACCECA[1], Vincent CHEVRIER[1], Viktor HOFFMANN[2], Jean-Pierre LORAND[3], Minoru FUNAKI[4], and Rupert HOCHLEITNER[5]

[1]CEREGE CNRS, Université d'Aix-Marseille 3, Aix en Provence, France
[2]Institute for Geosciences, University of Tübingen, Germany
[3]Mineralogy Department, Museum d'Histoire Naturelle, Paris, France
[4]National Institute of Polar Research, 9-10, Kaga 1-chome, Itabashi-ku, Tokyo 173-8515, Japan
[5]Mineralogical State Collection, Theresienstr. 41, 80333, Munich, Germany
[*]Corresponding author. E-mail: rochette@cerege.fr

(Received 17 May 2004; revision accepted 26 February 2005)

Abstract–Magnetic properties of 26 (of 32) unpaired Martian meteorites (SNCs) are synthesized to further constrain the lithology carrying Martian magnetic crustal sources. Magnetic properties of ultramafic cumulates (i.e., Chassigny, Allan Hills [ALH] 84001) and lherzolitic shergottites (ALH 77005, Lewis Cliff [LEW] 88516) are one or two orders of magnitude too weak to account for the crustal magnetizations, assuming magnetization in an Earth-like field. Nakhlites and some basaltic shergottites, which are the most magnetic SNCs, show the right intensity. Titanomagnetite is the magnetic carrier in the nakhlites (7 meteorites), whereas in most basaltic shergottites (11 meteorites) it is pyrrhotite. Dhofar (Dho) 378, Los Angeles, and NWA 480/1460 and 2046 are anomalous basaltic shergottites, as their magnetism is mainly due to titanomagnetite. Pyrrhotite should be among the candidate minerals for the magnetized Noachian crust.

INTRODUCTION

Understanding the origin of the huge Martian crustal magnetizations (Acuña et al. 1999) is a major challenge for Martian studies, both in terms of planetary dynamics and magnetic petrology. Present models for these anomalies require magnetization up to 15–30 A/m over a crustal thickness of 20–50 km (e.g., Langlais et al. 2004). Martian meteorites (hereafter called SNCs, including ALH 84001) (McSween and Treiman 1998) are our only direct samples available for the development of a magneto-mineralogical model for this crustal magnetization. Various arguments against their use have been raised recently (e.g., McSween 2002 and references therein). Apart from ALH 84001, the SNCs so far discovered, especially the shergottite group, are much younger (<1.2 Ga) than the inferred 4 Ga age of the Noachian magnetized crust. Locations of their sources on the planet are debated and the oversampling of young volcanic rocks (e.g., from Tharsis volcanoes, not representative of the old Noachian crust) was recently emphasized by McSween (2002). Other problems include the near-surface origin of SNCs (making it hard to use them to extrapolate to lower crustal levels) and their extensive shock metamorphism. However, it may be acceptable to assume that no major change in the Martian crustal petrogenetic features occurred from 4 Ga to less than 1 Ga. For comparison, most terrestrial basaltic rocks dating from 3 Ga to the present day have a similar magnetic mineralogy (around 1% of titanomagnetite) (e.g., Morimoto et al. 1997).

Here the origin of SNC magnetism will be discussed using an already published reappraisal that includes all desert finds up to the year 2000 (Rochette et al. 2001), together with the original data on all ANSMET Antarctic meteorites as well as the more recent Saharan finds: the NWA 817 and 998 nakhlites (Sautter et al. 2002) and the basaltic shergottites Dho 378 (Ikeda et al. 2002), NWA 480/1460, 856, 1068/1183/1775, 1195, 1669, and 2046 (Barrat et al. 2002a, 2002b; Jambon et al. 2002, 2003). Magnetic mineralogy data were implemented by a comprehensive petrographic data set on sulfide modal abundances and sulfide composition on nine samples (Lorand et al. Forthcoming). Including the already published magnetic studies (Cisowski 1986; Collinson 1986, 1997; Terho et al. 1991; Kirschvink et al. 1997; Funaki et al. 2002; Weiss et al. 2002; Antretter et al. 2003, Weiss et al. 2004), our synthesis will thus be based on 26 (of the 32 recognized so far) independent SNCs.

© The Meteoritical Society, 2005. Printed in USA.

METHODS AND SAMPLE DESCRIPTION

Original magnetic measurements have been performed on 0.02 to 0.8 g fragments, usually devoid of fusion crust (following Rochette et al. 2001). Samples were provided by NASA JSC (ALH, EET, LEW, MIL, QUE prefixes), the Theodore Monod consortium (NWA 480 and 817), MNHN Paris (Governador Valadares), B. and C. Fectay (NWA 856, 1068, 1669, 1950), A. Hupe (NWA 998 and 1195), E. Haiderer (Dho 378), M. Farmer (NWA 2046), and by P. Thomas (NWA 1775). Small fragments correspond to subsamples of the same meteorite so that average data from each meteorite or paired meteorites correspond to at least 0.3 g and up to several grams. In a few cases (Monod consortium samples), the measured sample was a polished section embedded in epoxy. This does not interfere with the quality of magnetic measurements but does give a 20% uncertainty on the sample mass. Hysteresis measurements were performed using a Micromag VSM, remanence measurements in a 2G cryogenic magnetometer equipped with DC SQUIDs, and low-field susceptibility with an Agico KLY-2. Remanence curves at low temperature were obtained in a MPMS cryogenic magnetometer (in IRM Minneapolis) and high-temperature susceptibility curves in a KLY3/CS3 system in INGV Roma. The S ratio is the isothermal remanent magnetization (IRM) obtained after applying a 3 T field and then a back field of –0.3 T normalized to the 3 T IRM. The IRM was imparted with a pulse magnetizer. Thermal demagnetization was performed under an Ar flux in an MMTD paleomagnetic oven. Data treatment for first order reversal curves (FORC) was performed using a software provided by C. Pike (Roberts et al. 2000). These FORC diagrams, useful for extracting more information from the hysteresis loop in interactions and mixtures of different grain sizes or minerals, will be applied for the first time to meteorites. New data obtained for this study are listed in Table 1, while Table 2 presents a synthesis of all available data. Natural remanence and magnetic anisotropy have been also investigated but results are presented in two other papers (Gattacceca et al. 2004, 2005).

MAGNETIC MINERALOGY OF MARTIAN ROCKS

Martian crustal magnetization has been proposed to be carried either by oxides (titanomagnetite or hematite) (Kletetschka et al. 2000) or sulfides (pyrrhotite) (Rochette et al. 2001). Both titanomagnetite and pyrrhotite are common minor ferrimagnetic phases in SNCs, while the other oxides described (chromite, ulvöspinel, and ilmenite) are typically paramagnetic (although Weiss et al. [2002] report ferromagnetic chromite in ALH 84001). Hematite has not been detected in SNCs or identified in thin sections and is highly unlikely to be present in lower crustal Martian rocks due to the high oxidation level it implies compared to that inferred for the Martian mantle and uncontaminated volcanic rocks (FMQ –1 to –3 log units) (Xirouchakis et al. 2002). The occurrence of hematite-bearing lower crustal rocks on Earth (McEnroe et al. 2002) may be attributed to the orogenic recycling of oxidized surface material, a process likely absent on Mars. The detection of hematite on Mars via remote sensing has been interpreted as indicative of sedimentary deposits (Christensen et al. 2001) and is thus unrelated to an igneous mineral assemblage.

Generally good consistency is found in the magnetic parameters (related both to the nature and amount of magnetic minerals) among different fragments of the same meteorite or among paired meteorites (DaG 476/489/670/1037, NWA 1068/1183/1775 or 480/1460, SaU 004/0990) (Rochette et al. 2001, present Table 1, and "s.d." column in Table 2). This indicates that the mineralogy is quite homogeneous even at the fraction of a gram sample scale and confirms pairing among the DaG, NWA, and SaU multiple finds. Only Los Angeles (Rochette et al. 2001) and Dho 378 (this study) show highly variable amounts of ferrimagnetic grains, though with consistent mineralogy.

Both low- and high-Ti titanomagnetite as well as pyrrhotite have been identified in SNCs using various techniques and mineralogical investigations (McSween and Treiman 1998; Rochette et al. 2001; Lorand et al. Forthcoming). Pyrrhotite is abundant in shergottites and very rare in nakhlites. In all basaltic shergottites (except Dho 378, Los Angeles, and NWA 480/1460 and 2046) high coercivity pyrrhotite is easily identified by a combination of hysteresis parameters (Fig. 1; $B_{cr} > 80$ mT, B_{cr}/B_c and M_{rs}/M_s typical of pseudo-single domain [PSD] to single domain [SD] state) as well as by an S ratio > –0.9. Another criteria for pyrrhotite, $\mu_o M_{rs}/\chi_f \geq B_{cr}$ (Rochette et al. 1990; Peters and Thompson 1998) is satisfied by these rocks (Table 1). However, some titanomagnetite-bearing SNCs also exhibit the same relation. The unblocking of 80% of the IRM below 350 °C (Fig. 2) and the FORC diagram for NWA 1068 (Fig. 3a) are clearly incompatible with (titano-)magnetite (Roberts et al. 2000) and are typical of pyrrhotite (Wehland et al. Forthcoming). The amount of pyrrhotite, with estimates from modal analysis and saturation magnetization (Rochette et al. 2001), varies from 0.1 to 1 wt%. A more or less minor soft component is observed in finds (except NWA 1068) and could be due to titanomagnetite or coarse-grained multidomain (MD) pyrrhotite. The latter is possibly linked to terrestrial alteration. This soft component is most pronounced in NWA 1669, which exhibits a coercivity characteristic of magnetite and an S ratio characteristic of a hard mineral, here interpreted as pyrrhotite. This mixture is well evidenced by the wasp-waisted hysteresis loop (Fig. 1b). On the FORC diagram (Fig. 3c) the signature of PSD magnetite dominates, though the elongation toward high B_c values can be attributed to pyrrhotite. In that sample, magnetite is most likely linked to remnants of fusion crust, which are visible on one side. Such

Table 1. Original new measurements of magnetic properties of Martian meteorites. Several chips were measured for some Antarctic meteorites and listed separately. Low and high field susceptibilities (χ_o and χ_h) are in 10^{-9} m^3/kg, saturation magnetization (M_{rs}) in 10^{-3} Am^2/kg, and coercive field (B_{cr}) in mT. Median destructive field (MDF) was obtained by 3 axis AF demagnetization of a 3 T IRM, while coercive fields are measured with a 1 T saturating field.

	χ_o	χ_{hf}	M_{rs}	MDF (mT)	M_{rs}/M_s	B_{cr} (mT)	B_{cr}/B_c	S ratio	Mass (mg)
Basaltic shergottites									
DaG 1037	794	162	17.4	65	0.36	86	2.08	–0.81	239
EET A79001A	675	525	17.9	48	0.33	69	1.73	–0.79	222
EET A79001B.1	886	340	28.5	58	0.37	82	1.95	–0.60	67
EET A79001B.2	803	363	23.4	67	0.36	91	2.12	–0.62	150
EET A79001B.2	1118	402	26.6	55	0.4	78	1.90	–0.64	88
NWA 856	943	463	17.1		0.37	113	1.98	–0.82	289
NWA 1068	1262	367	99.4	100	0.47	134	1.54	–0.74	320
NWA 1183	1586	407	131	75	0.43	121	1.53	–0.68	816
NWA 1195	1315	293	23.0	80	0.32	122	2.80	–0.90	698
NWA 1775	1622	557	154	90	0.50	128	1.48	–0.73	136
NWA 1669	1600	427	59.0	40	0.39	53	1.70	–0.82	227
QUE 94201	1305	358	55.6	67	0.43	92	1.70	–0.90	320
SaU 090	766	288	6.4	65	0.23	80	3.89	–0.78	687
Dho 378.1	1916	444	53.5	18	0.27	55	2.20	–0.94	15
Dho 378.2	4618	263	15.7	10	0.09	20	6.11	–0.90	753
NWA 480	2920	430	102		0.33	61	1.69	–0.96	640
NWA 1460	2661	490	126	42	0.30	64	1.80	–0.93	70
NWA 2046	2765	411	21.6	35	0.22	36	4.32	–0.92	80
Nakhlites									
Governador Valadares	2280	521	89.7	37	0.32	60	1.78	–0.95	376
MIL 03346	5128	470	398	32	0.32	58	1.56	–0.99	464
NWA 817	5903	249	133		0.27	56	1.75	–0.98	500
NWA 998.1	4256	427	171	25	0.24	41	1.73	–0.98	849
NWA 998.2	3750		162	24				–0.99	860
Ultramafics									
ALH A77005.1	2965	564	10.6	25	0.18	21.8	4.84	–0.99	128
ALH A77005.2	1873	536	8.4	25	0.19	26.5	3.53	–1	110
ALH 84001	647	351	1.50	27	0.26	40	2.35	–0.93	209
LEW 88516.1	2660	427	26.0	54	0.27	63	4.32	–0.90	70
LEW 88516.2	2701	369	29.3	33	0.28	50	2.94	–0.94	45
LEW 88516.3	1995	199	16.4	40	0.22	49	2.88	–0.91	41
NWA 1950	5770								1530

soft component is also marked on the fine-grained lithology A of EET A79001, while the coarse-grained lithology B is more typical of other pyrrhotite-bearing shergottites, which is in agreement with the current interpretation of these lithologies (McSween and Treiman 1998).

The magnetic properties of the seven studied nakhlites are quite similar and suggest nearly PSD titanomagnetite (S <–0.95, B_{cr}/B_c and M_{rs}/M_s near 1.7 and 0.3, respectively) (Table 2 and Fig. 1a). This agrees with previous thin section studies (Rochette et al. 2001) and the new petrographic data for NWA 817 which all indicate very low sulfide/titanomagnetite modal ratios (<0.01). However, significant amounts of pyrrhotite are found in Y-593. High Curie points (530–580 °C) characterize Nakhla (e.g., Shaw et al. 2001) and Y-593 (Funaki et al. 2002). Compared to the rather large Ti content reported by microprobe analysis for nakhlites, this suggests that the titanomagnetites bear exsolved Ti-poor lamellae (as observed in Y-593). MIL 03346 appears to be the most magnetic nakhlite, with nearly five times more magnetite per unit mass than the more weakly magnetic set (Nakhla, Governador Valadares, Lafayette, and Y-593).

Four basaltic shergottites (Dho 378, Los Angeles, NWA 480/1460, and NWA 2046) are similar in terms of magnetic properties to nakhlites, although they contain abundant pyrrhotite according to thin section examinations. This pyrrhotite is either antiferromagnetic, or MD with a minor contribution to total remanent magnetization. In Dho 378 and NWA 2046, the S ratio and wasp-waisted loop (as well as the composite back field remanence curve) (Fig. 4) suggest a minor contribution of pyrrhotite to saturation remanence. A Curie point of 150 °C has been reported for Los Angeles (Rochette et al. 2001), similar to what can be

Table 2. Mean magnetic properties of Martian meteorites. See Table 1 for parameter definition. Standard deviation (s.d.) is provided only for χ_o and M_{rs}.

	χ_o	s.d.	χ_{hf}	M_{rs}	s.d.	M_{rs}/M_s	B_{cr}	B_{cr}/B_c	S ratio	Weight % pyrrhotite[a]
Basaltic shergottites										
DaG 476/489/670/1037[b, c]	707	167	358	18.6	4.2	0.34	94	2.60	–0.86	0.29
Dho 019[c]	579	73	430	23.1		0.36	81	1.59	–0.87	
EET A79001A[b, d]	653	32	525	18.0	4.0	0.33	69	1.73	–0.79	
EET A79001B[b]	936	163	368	25.3	2.9	0.38	84	1.99	–0.62	
NWA 856[b]	752	167	463	17.1		0.37	113	1.98	–0.82	
NWA 1068/1183/1775[b]	1435	193	443	128	27	0.45	128	1.51	–0.72	1.0
NWA 1195[b]	1315		293	23.0		0.32	122	2.80	–0.90	
NWA 1669[b]	1600		427	59.0		0.39	53	1.70	–0.82	
QUE 94201[b]	1305		358	55.6		0.43	92	1.70	–0.9	
SAU 005/0990[b, c]	766	119	295	5.27	0.98	0.22	92	4.38	–0.63	0.21
Shergotty[c, d]	757	76	476	27.9	6.4	0.38	113	1.82	–0.72	0.29
Zagami[c, d]	510	89	399	10.7	4.2	0.36	97	1.62	–0.83	0.53
Los Angeles[c]	5743	3970	719	360	353	0.49	55	1.41	–1	0.45
NWA 480/1460[b]	2791	183	460	117	13	0.32	62	1.74	–0.95	0.16
Dho 378[b]	3567	1486	353	34.6	26.7	0.18	37	4.16	–0.92	
NWA 2046[b]	2765		411	21.6		0.22	36	4.32	–0.92	
Nakhlites										
Governador Valadares[b, d]	1945	474	521	89.7	12.8	0.32	60	1.78	–0.95	
Lafayette[d]	2101	959		69.0	12.5					
MIL 03346[b]	5128		470	398		0.32	58	1.56	–0.99	
Nakhla[c, d]	1482	171	420	77.4	10.2	0.3	61	1.79	–0.97	0.04
NWA 817[b]	5903		249	133		0.27	56	1.75	–0.98	0.02
NWA 998[b]	4256		427	171		0.24	41	1.73	–0.98	
Y-000593[d]	4400			73.0		0.11	31	4.60		
Ultramafics										
ALH A77005[b, d]	2419	772	564	10.0	3.8	0.18	24	4.20	–0.99	
ALH 84001[b, d]	647		351	1.50	0.40	0.26	40	2.35	–0.90	<0.03
Chassigny[c, d]	562		554	0.68	0.16	0.11	63	2.33	–0.95	0.015
LEW 88516[b]	2452	396	332	23.5	7.1	0.26	54	3.38	–0.92	

[a]Derived from modal analysis (Lorand et al.) or from S content (McSween and Treiman 1998).
[b]Data provenance is from Table 1.
[c]Data provenance is from Rochette et al. (2001).
[d]Data provenance is from literature:
Cisowsky (1986): ALH 77005, EET A79001a, Governador Valadares, Nakhla, Shergotty, and Zagami.
Collinson (1986): ALH 77005 and EET A79001a.
Collinson (1997): Chassigny, Governador Valadares, Lafayette, Nakhla, ALH 84001, Shergotty, and Zagami.
Terho et al. (1991): EET A79001a and Zagami.
Funaki et al. (2002): Y-000593.
Antretter et al. (2003): ALH 84001.

extrapolated according to the composition of NWA 480 titanomagnetite (Barrat et al. 2002a). A specific petrogenesis should account for the lower Ti content of the titanomagnetites of these four compared to the other basaltic shergottites, where paramagnetic high-Ti titanomagnetite is usually reported as ulvöspinel. Until now, we have used the "basaltic shergottite" category in a broad sense (following McSween and Treiman 1998 and McSween 2002), i.e., including the "olivine-phyric" (or "picritic") and "basaltic" stricto sensu categories (according to Goodrich 2002 and Barrat et al. 2002b). However, it is worth noting that the titanomagnetite-bearing cases are encountered only in the basaltic stricto sensu category (except NWA 2046), while all olivine-phyric (except NWA 2046) and the majority of basaltic stricto sensu shergottites have their saturation remanence controlled by pyrrhotite.

The lherzolitic shergottite ALH A77005 and Chassigny yield magnetic properties of soft (titano-)magnetite (i.e., coarser-grained than in nakhlites). Since they contain 1.5–3 vol% of Fe^{3+}-bearing chromites, it is likely that magnetite is present as inclusions in the chromite grains. A mixture of soft and hard phases, possibly magnetite and pyrrhotite, is suggested by wasp-waisted hysteresis loops (Fig. 1b) as well as by the S values in ALH 84001 and LEW 88516. Indeed,

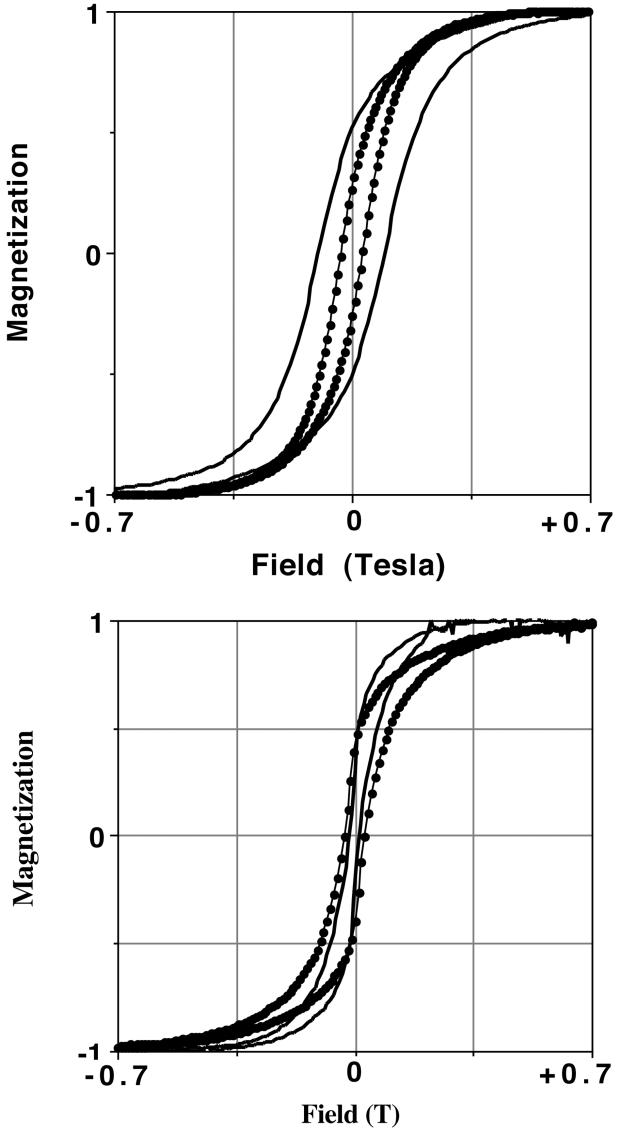

Fig. 1. Hysteresis loops corrected for high field slope (fitted in the 0.7 to 1 T range): a) single mineral loops for NWA 817 (magnetite = circles) and NWA 1068 (pyrrhotite = no symbols); b) wasp-waisted loops for LEW 88516 (no symbols) and NWA 1669 (circles), which is indicative of a magnetite/pyrrhotite mixture.

pyrrhotite has been observed in thin sections of the lherzolitic shergottites. We were able to measure only χ_o of the new lherzolitic shergottite, NWA 1950: 58 10^{-7} m^3/kg. This very high value indicates that this meteorite is about two times richer in magnetite than the other lherzolitic shergottites (Table 2), which is possibly linked to serpentinization. ALH 84001's complex magnetic properties probably require multiple magnetic carriers (SD magnetite in the carbonate blebs, pyrrhotite, and possibly inclusions in chromite) in debatable proportions (Weiss et al. 2002, 2004; Antretter et al. 2003). The FORC diagram of our ALH 84001 sample (Fig. 3b) indicates a dominant mixture of PSD and SD

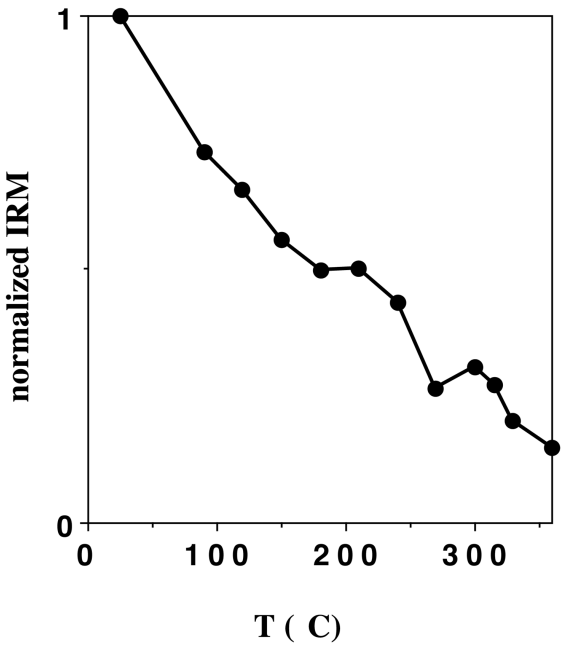

Fig. 2. Normalized saturation remanence (IRM) versus demagnetization temperature (under Ar flow) for the NWA 1068 shergottite.

magnetite. However, there is clear evidence that SD magnetite in carbonates is a secondary impact-induced mineral in ALH 84001 (e.g., Barber and Scott 2002), so that pyrrhotite and chromite may appear to be the primary magnetic minerals in the only Martian meteorite of Noachian age.

In terms of low field magnetic susceptibility χ_o, the categories highlighted above are well defined: the pyrrhotite-bearing shergottites, as well as Chassigny and ALH 84001, have weak χ_o (5 to 14 $10^{-7}m^3$/kg). The titanomagnetite-bearing basaltic and lherzolitic shergottites as well as the nakhlites have higher values (16 to 59 $10^{-7}m^3$/kg). On the other hand, high field susceptibility (defined using the Micromag in the 0.7 to 1 T range), mainly due to paramagnetic iron in silicates, is similar for all SNCs (3 to 7 $10^{-7}m^3$/kg).

REMANENCE INTENSITY

In situ natural remanent magnetization (NRM) intensity depends on the amount, type, and grain size of magnetic mineral, magnetization process, and ambient field intensity during acquisition. To account for the intensity of crustal NRM, as well as its depth and its stability since 4 Gyr, one may assume a thermoremanence (TRM) acquisition in an Earth-like internal dynamo magnetic field (about 50 μT). Chemical remanence (CRM) could also be a viable acquisition mechanism because it can be of the same order as TRM (McClelland 1996). SNC NRM is not the correct analog

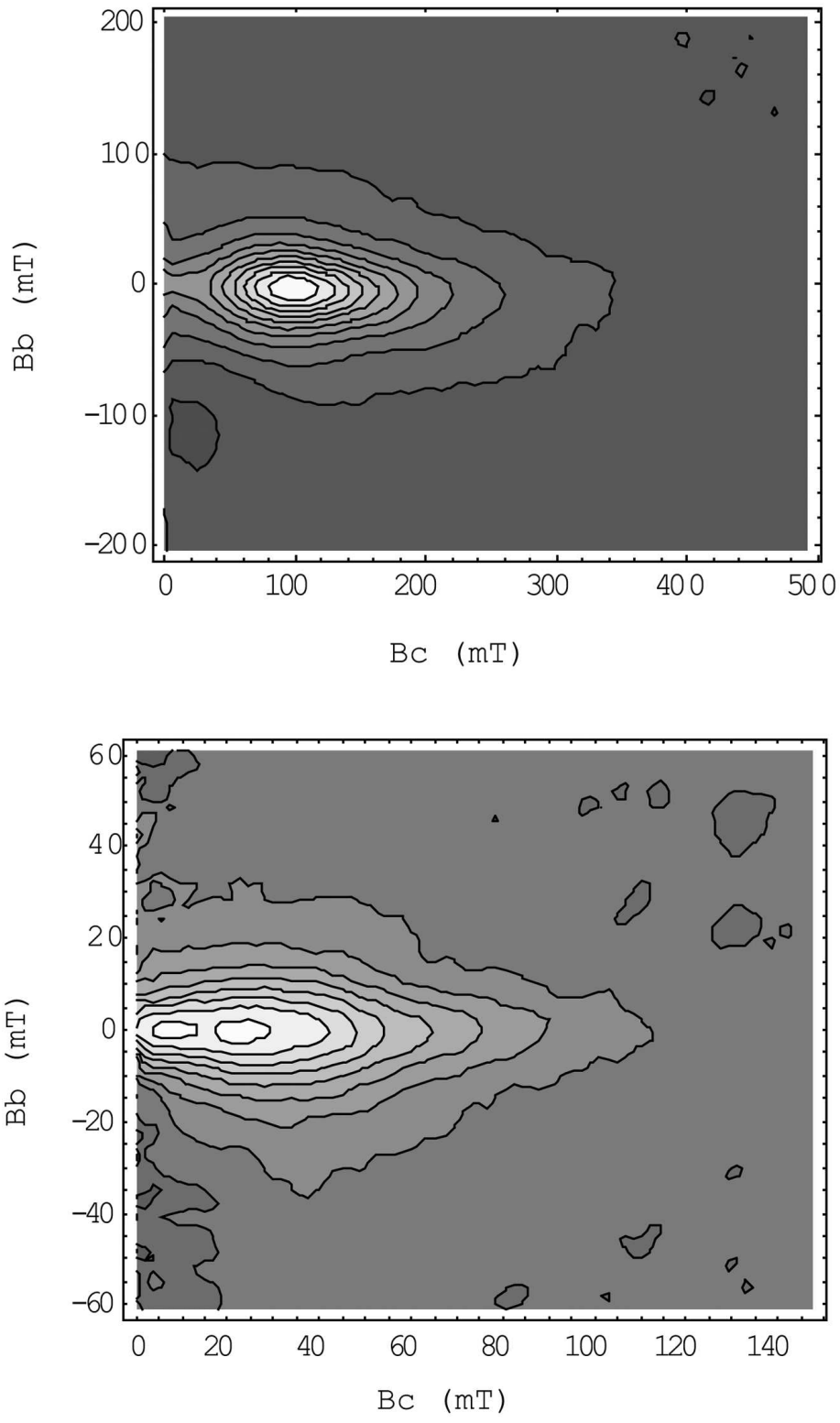

Fig. 3. First order reversal curves (FORC) diagrams of a) NWA 1068 (smoothing factor SF = 3), b) ALH 84001 (SF = 5).

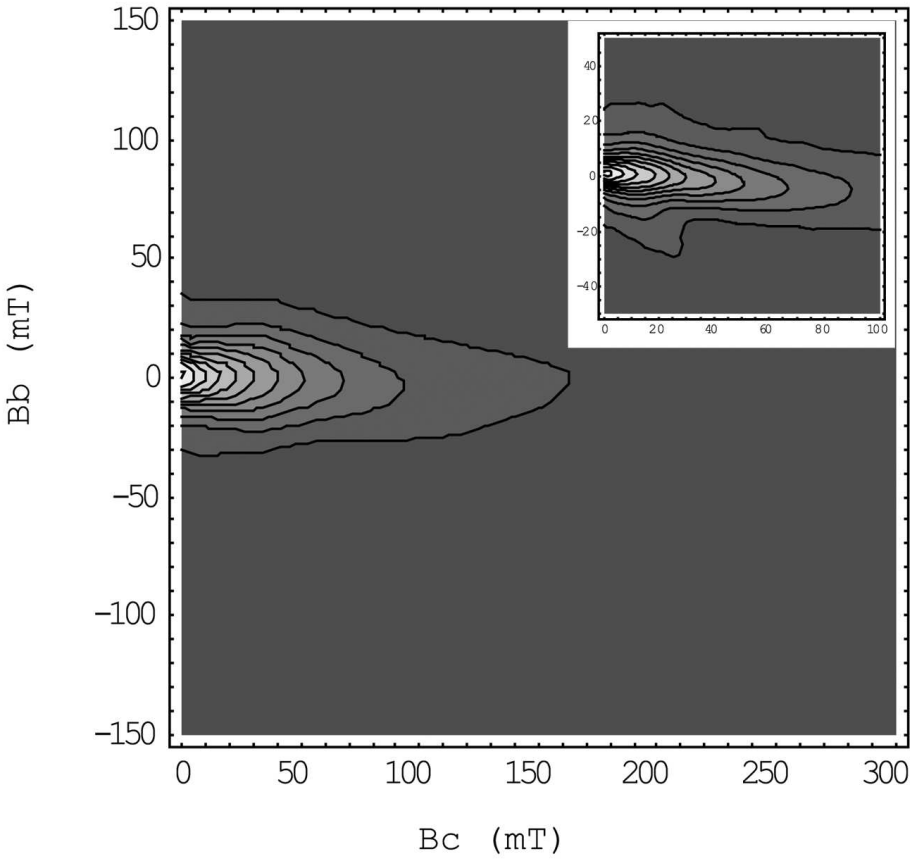

Fig. 3. *Continued.* First order reversal curves (FORC) diagram of c) NWA 1669 (SF3). The insert in (c) shows a more detailed diagram limited to $B_c < 100$ mT.

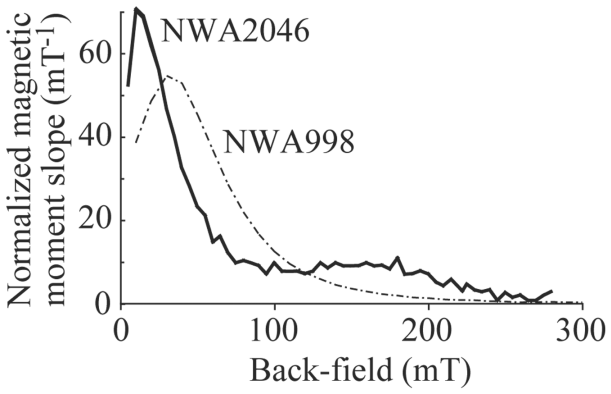

Fig. 4. The absolute value of the derivative of the backfield remanence curve, measured on the Micromag VSM on NWA 2046 and compared to NWA 998.

for the highly magnetized Martian crust as the few paleointensity studies (Cisowski 1986; Collinson 1997; Shaw et al. 2001; Gattacceca et al. 2004) suggest an acquisition field an order of magnitude lower than 50 μT and aquired after the dynamo shutdown and/or via a non-TRM acquisition process. Indeed, SNCs have been more likely magnetized during or after impact than during the initial magmatic cooling. Therefore, it is more significant to estimate the in situ NRM for the Noachian equivalents of SNCs by using their saturation IRMs and the proposed upper bound of 2% for NRM/IRM in case of TRM in an Earth-like field for magnetite or pyrrhotite (Kletetschka et al. 2003). Taking 5 A/m for the minimal crustal NRM (e.g., Parker 2003) and a mass density of 3 leads to a minimum saturation IRM of 83 10^{-3} Am^2/kg (Fig. 5). Only four nakhlites (Governador Valadares, MIL 03346, and NWA 817 and 998), two titanomagnetite-bearing basaltic shergottites (Los Angeles and NWA 480/1460), and one pyrrhotite-bearing shergottite (NWA 1068/1183/1755) exceed this threshold. A few other basaltic shergottites and the other nakhlites are just below the threshold. ALH 84001, the only SNC of Noachian age, is two orders of magnitude below (with concordant IRM values between this study and Weiss et al. 2002 or Antretter et al. 2003), similar to Chassigny. Lherzolitic shergottites and the remaining basaltic shergottites are nearly one order of magnitude below the threshold. This may imply that the magnetic sources are rather mafic than ultramafic rocks. The scenario of a crustal magnetization due to magnetite formed by siderite breakdown (Scott and Fuller 2004), by analogy

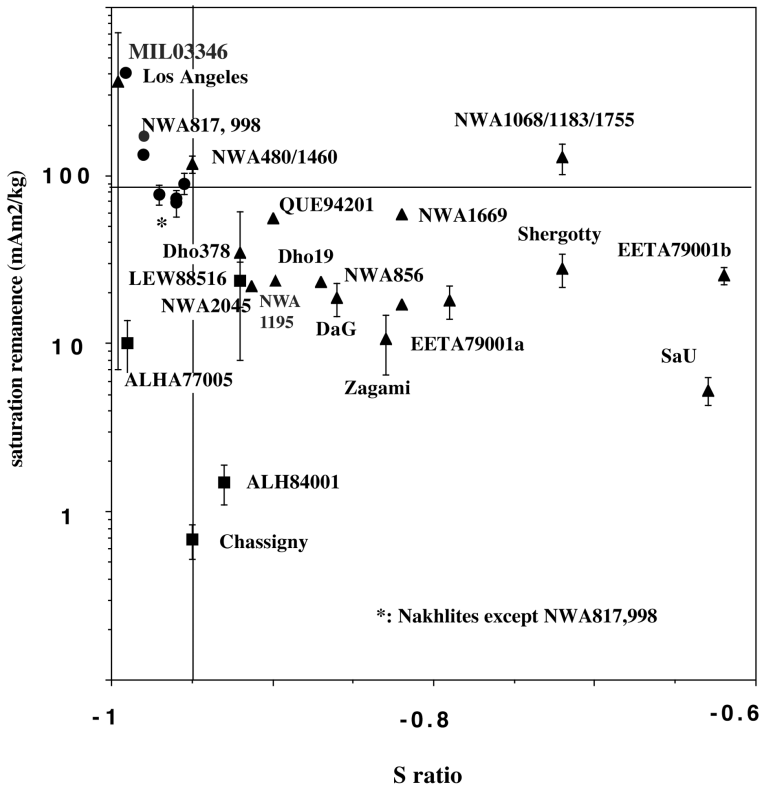

Fig. 4. The absolute value of the derivative of the backfield remanence curve, measured on the Micromag VSM on NWA 2046 and compared to NWA 998.

with ALH 84001, is undermined by the very low IRM of ALH 84001.

Our magnetic susceptibility database also allows us to estimate the possible contribution of induced magnetization to Martian magnetic anomalies. Surface magnetic fields in the range of 1–10 μT can be predicted over the most magnetic parts of the Noachian crust (e.g., Langlais et al. 2004). The observed magnetic susceptibilities, which are in the range of 1.5 to 18 10^{-3} SI (converted in volume unit from Table 2), thus correspond to an induced magnetization in the range of 10^{-3}–10^{-1} A/m, which is negligible compared to the required crustal magnetization. However, we cannot exclude the possibility that future low-altitude or ground magnetic survey could reveal induced magnetic anomalies in the Martian subsurface.

DISCUSSION AND CONCLUSIONS

Although some nakhlites show the appropriate magnetic properties, their peculiar petrography does not fit with the averaged Martian crust (McSween 2002). Moreover, their large M_{rs}/M_s ratio (PSD-like, in contradiction with the large grain size) may be shock induced or linked to the shallow emplacement and not representative of deeper unshocked rocks. The Curie point of 150 °C found in Los Angeles and inferred in NWA 480/1460 and Dho 378 from electron microprobe is at odds with a Curie depth of 20–50 km during NRM acquisition. Although this depth is hard to evaluate precisely, the temperature range reached at a depth of 20–50 km in early Mars should be 300–600 °C according to Nimmo and Gilmore (2001). On the other hand, pyrrhotite, with its Curie point of 325 °C, can account for the anomalies, provided that Noachian crustal rocks are richer in sulfides than the average basaltic shergottites (at least 1 wt%). Alternatively, one could invoke an early Martian field much stronger than the 50 μT used in our estimations. Noachian crust is likely to be richer in pyrrhotite than terrestrial crust for several reasons: 1) sulfates are abundant in Martian soils; 2) the Noachian mafic-ultramafic crust is thought to have crystallized from FeO-rich basalts, which according to current experiments (O'Neill and Mavrogénes 2002) could have dissolved twice as much FeS from the mantle than their terrestrial counterparts; and 3) Martian and terrestrial crusts are expected to have different sulfide mineralogy: pyrrhotite is the stable Fe sulfide for fO_2 < FMQ while pyrite (paramagnetic) is more widespread in the oxidized terrestrial crust (see discussion in Rochette et al. 2001). Another argument for pyrrhotite as the preferred candidate mineral for Martian crustal magnetization is the observed crater demagnetization (Nimmo and Gilmore 2001; Hood et al.

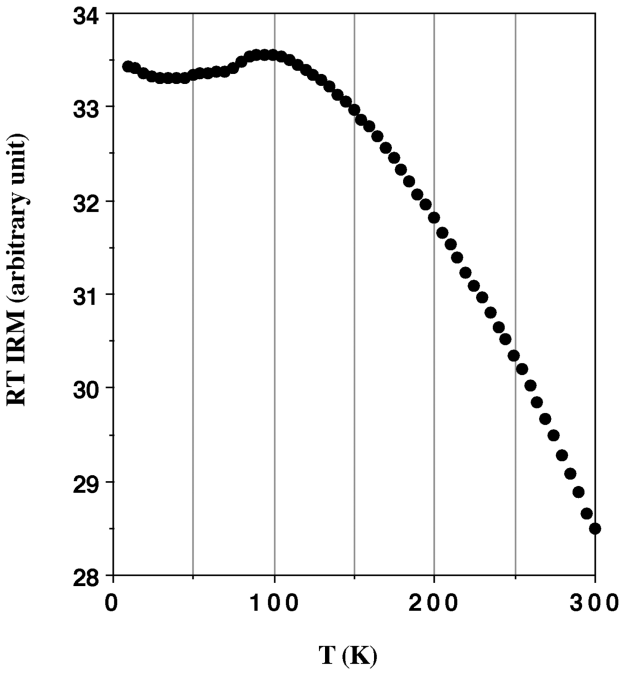

Fig. 6. The cooling curve of IRM acquired at room temperature (MPMS IRM Mineapolis) for NWA 1068. The hump near 100 K is likely due to ordering of chromite (Rochette et al. 2001; Anttreter et al. 2003; Weiss et al. 2004).

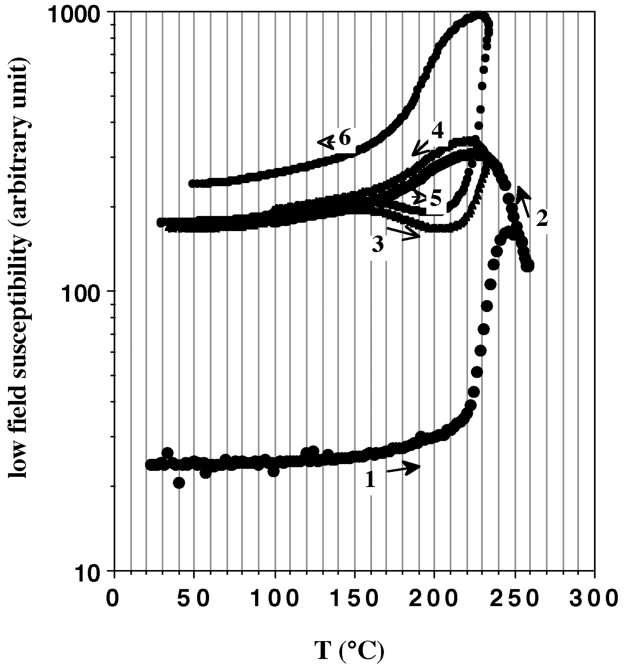

Fig. 7. Successive runs of susceptibility versus temperature under Ar flow (using CS3-KLY3 in INGV, Roma, Italy) for an hexagonal pyrrhotite sample showing very low initial susceptibility, and complex behavior around the transition. In the third run, temperature was maintained at 230 °C for 10 minutes.

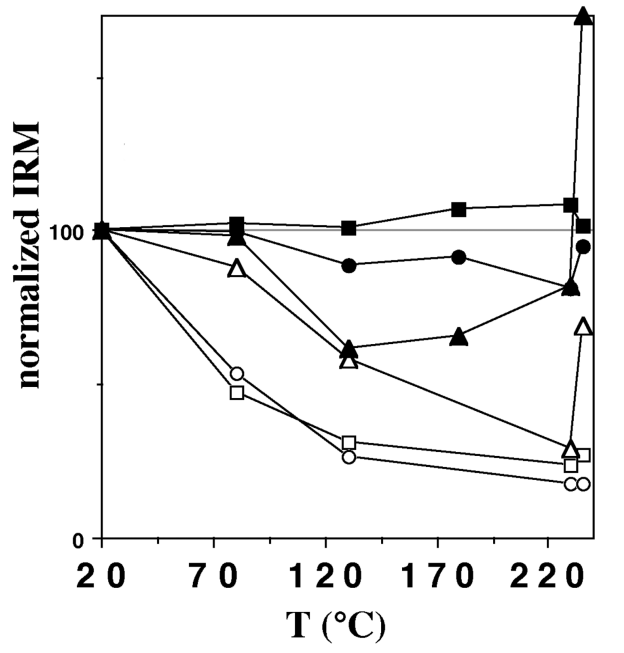

Fig. 8. Residual IRM (open symbols) versus demagnetization temperature for Shergotty (squares), Zagami (circles), and quenched hexagonal pyrrhotite (triangles) with value of resaturated IRM after heating (closed symbols). The cooling rate is slow (<50 °C per hour), except for the last point (at 230 °C but plotted at 235 °C for clarity) for which the heating tube has been quenched.

2003), which can be explained by a simple mechanism in the case of pyrrhotite. At room temperature, this mineral exhibits a magnetic transition from the ferrimagnetic to paramagnetic state near 2.8 GPa (Rochette et al. 2003), implying that Noachian NRM will be erased for the crustal volume submitted to a higher pressure during impact. It also implies that no pre-shock magnetic memory was left in pyrrhotite-bearing shocked SNCs, which justifies our assertion that SNC NRMs are not relevant to the discussion of Martian crustal magnetizations.

On the other hand, Rochette et al. (2001) and Lorand et al. (Forthcoming) suggest that pyrrhotite in SNCs should be mostly the antiferromagnetic (AF) hexagonal polymorph (Fe_9S_{10}). Further experiments confirm this assertion. The low main unblocking temperature of NWA 1068 (Fig. 2) in particular, as well as the lack of low temperature transition at 34 K (Rochette et al. 2001 and Fig. 6), do not point toward a regular monoclinic pyrrhotite (Rochette et al. 1990). The presence of a ferrimagnetic (FE) metastable hexagonal form has been attributed to shock, quenching, or irradiation damages on the hexagonal structure. Such an FE hexagonal pyrrhotite can be obtained by quenching a natural sample of AF Fe_9S_{10} from above the λ transition at 200–220 °C (Bennet and Graham 1981). This is exemplified in Fig. 7, which shows susceptibility χ versus temperature cycles for an hexagonal pyrrhotite sample initially in the AF state. During the first heating, χ increases rapidly above the λ transition, due to

appearance of the FE state, then decreases while approaching the Curie point. During cooling, the FE phase only partly reverts to the AF phase. Subsequent reheatings (3 and 5) activate the metastable FE to AF conversion in the 150–200 °C range (below the λ transition). Holding the temperature at 230 °C results in creating more of the FE phase above the λ transition and thus more metastable FE phase at room temperature (branch 6).

We compared the thermal behavior of Zagami and Shergotty with that of quenched hexagonal pyrrhotite prepared by dispersing powder (the same material as in Fig. 7, quenched from 230 °C) in a high-temperature cement. Shergotty and Zagami show large IRM unblocking at low temperatures (Fig. 8), which again is not typical of fine-grained monoclinic pyrrhotite. The new IRM acquired after heating and slow cooling (20 deg/hr) at different steps from 80 to 230 °C, as well as quenching from 230 °C, shows for the quenched hexagonal pyrrhotite the expected behavior when crossing the λ transition (closed triangles in Fig. 8). First, a decrease is observed due to the relaxation of the metastable FE state into the AF state, and then a particularly large increase for the last rapid cooling run due to the appearance of new FE structures. Zagami (but not Shergotty) does show a similar behavior, although less pronounced. Therefore, the FE pyrrhotite observed in SNCs may be at least partly equivalent to a quenched hexagonal polymorph, although we acknowledge that the actual magnetic state of pyrrhotite in shergottites remains unclear. Of likely importance in that open question are the high Ni content and exsolved pentlandite lamellae in SNC pyrrhotites (Lorand et al. Forthcoming). It is worth noting that shock-induced magnetic phase transition in pyrrhotite has been invoked by Shi and Tarling (1999).

One may also consider the alternative that ferrimagnetic chromite may account for the magnetic properties, here attributed to pyrrhotite (Yu, personal communication; Yu et al. 2001). However, the composition necessary to observe a high Curie point (e.g., 260 °C for a $Fe_{1.9}Cr_{1.1}O_4$ in Yu et al. 2001) differs strongly from the typical composition of chromite in shergottites ($Fe_{1.6}Cr_{0.9}Al_{0.3}Mg_{0.2}O_4$ in McSween and Treiman 1998). This latter composition corresponds to paramagnetic chromite with Néel point near 90 K (Weiss et al. 2004). Moreover, chromite is absent or very rare in basaltic shergottites.

If the ferrimagnetism of pyrrhotite in SNCs is linked to a specific metastable state, the equivalent Martian crustal rocks in situ may not bear ferrimagnetic pyrrhotite. However, the actual pyrrhotite polymorph at depth is difficult to assess. In the KTB deep hole (down to 9 km), monoclinic pyrrhotite is the major magnetic phase down to 8 km (230 °C) and is responsible for a surface magnetic anomaly. Below 8 km, it is replaced by the AF hexagonal form (Kontny et al. 2000). The KTB case suggests a rather shallow demagnetization of pyrrhotite-bearing crustal rocks, but the equivalent Martian depth for the same temperature is much larger. The presence of high-temperature hexagonal pyrrhotite polymorphs in SNCs may be linked to the fast cooling of these rocks, while monoclinic pyrrhotite structure could dominate in slowly cooled deep rocks.

Although fundamental drawbacks exist in the use of SNCs to put forward a magneto-mineralogical model for magnetic anomalies, sulfides appear as a serious alternative to oxides in the Martian case. This conclusion is based on several facts:

1. Pyrrhotite is present in practically all SNCs, including ALH 84001;
2. Pyrrhotite magnetic signature dominates in the most common strongly magnetic Martian lithology—basaltic shergottites;
3. Pyrrhotite provides an efficient mechanism for impact demagnetization; and
4. Pyrrhotite shows a larger Curie depth than the titanomagnetite encountered in some other basaltic SNCs. However, this hypothesis suffers from the identification of the hexagonal form rather than the monoclinic form of pyrrhotite in SNCs.

Acknowledgments–We are indebted to the numerous persons and institutions who provided rare samples for this study, particularly to the Meteorite Working Group for approving our ANSMET sample request, to C. Satterwithe from NASA JSC, to J. A. Barrat, A. Jambon, and V. Sautter from Théodore Monod consortium, to E. Haiderer and A. Hupé, and to the rock magnetic laboratories of IRM Minneapolis (M. Jackson) and INGV Roma (L. Sagnotti). B. Weiss, an anonymous reviewer, and K. Righter helped us to improve the original manuscript. This work was supported by the INSU-CNES Planetology program.

Editorial Handling— Dr. Kevin Righter

REFERENCES

Acuña M. H., Connerney J. E. P., Ness N. F., Lin R. P., Mitchell D., Carlson C. W., McFadden J., Anderson K. A., Reme H., Mazelle C., Vignes D., Wasilewski P., and Cloutier P. 1999. Global distribution of crustal magnetization discovered by the Mars Global Surveyor MAG/ER experiment. *Science* 284:790–793.

Antretter M., Fuller M., Scott E., Jackson M., Moskowitz B., and Solheid P. 2003. Paleomagnetic record of Martian meteorite ALH 84001. *Journal of Geophysical Research* 108:doi:10.1029/2002JE001979.

Barber D. and Scott E. 2002. Origin of supposedly biogenic magnetite in the Martian meteorite Allan Hills 84001. *Proceedings of the National Academy of Sciences* 99:6556–6561.

Barrat J. A., Gillet P., Sautter V., Jambon A., Javoy M., Göpel C., Lesourd M., Keller F., and Petit E. 2002a. Petrology and chemistry of the basaltic shergottite Northwest Africa 480. *Meteoritics & Planetary Science* 37:487–499.

Barrat J. A., Jambon A., Bohn M., Gillet P., Sautter V., Göpel C., Lesourd M., and Keller F. 2002b. Petrology and chemistry of the picritic shergottite Northwest Africa 1068 (NWA 1068). *Geochimica et Cosmochimica Acta* 66:3505–3518.

Bennet C. E. G. and Graham J. 1981. New observations on natural pyrrhotites: Magnetic transition in hexagonal pyrrhotite. *American Mineralogist* 66:1254–1257.

Christensen P. R., Morris R. V., Lane M. D., Bandfield J. L., and Malin M.C. 2001. Global mapping of Martian hematite mineral deposits: Remnants of water-driven processes on early Mars. *Journal of Geophysical Research* 106:23,873–23,885.

Cisowsky S. M. 1986. Magnetic study on Shergotty and other SNC meteorites. *Geochimica et Cosmochimica Acta* 50:1043–1048.

Collinson D. W. 1986. Magnetic properties of Antarctic shergottite meteorites EET A79001 and ALH A77005: Possible relevance to a Martian magnetic field. *Earth and Planetary Science Letters* 77:159–164.

Collinson D. W. 1997. Magnetic properties of Martian meteorites. *Meteoritics & Planetary Science* 32:803–811.

Funaki L., Hoffmann V., and Fukuma K. 2002. The meaning of unstable remanent magnetization of Y-000593 (abstract). *Antarctic Meteorites* 27:23–24.

Gattacceca J. and Rochette P. 2004. Toward a robust relative paleointensity estimate in meteorites. *Earth and Planetary Science Letters* 227:377–393.

Gattacceca J., Rochette P., Denise M., Consolmagno G., and Folco L. 2005. An impact origin for the foliation of ordinary chondrites. *Earth and Planetary Science Letters,* 234:351–368, doi:10.1016/j.epsl.2005.03.002.

Goodrich C. A. 2002. Petrogenesis of olivine-phyric shergottites Sayh al Uhaymir 005 and Elephant Moraine A79001 lithology A. *Geochimica et Cosmochimica Acta* 67:3735–3772.

Hood L., Richmond N. C., Pierazzo E., and Rochette P. 2003. Distribution of crustal magnetic fields on Mars: Shock effects of basin-forming impacts. *Geophysical Research Letters* 30, doi: 10.1029/2002GL016657.

Ikeda Y., Takeda H., Kimura M., and Nakamura N. 2002. A new basaltic shergottite, Dhofar 378 (abstract). *Antarctic Meteorites* 27:40–42.

Jambon A., Barrat J. A., Sautter V., Gillet P., Göpel C., Javoy M., Joron J-L., and Lesourd M. 2002. The basaltic shergottite Northwest Africa 856: Petrology and chemistry. *Meteoritics & Planetary Science* 37:1147–1164.

Jambon A., Bohm M., Boudouma O., Chennaoui-Aoudjehane H., and Franchi I. 2003. Al Mala'ika (NWA 1669): A new shergottite from Morocco: Mineralogy and petrology (abstract). *Meteoritics & Planetary Science* 38:A43.

Kirschvink J. L., Maine A. T., and Vali H. 1997. Paleomagnetic evidence of a low temperature origin of carbonate in the martian meteorite ALH 84001. *Science* 275:1629–1631.

Kletetschka G., Wasilewski P. J., and Taylor P. T. 2000. Mineralogy of the source for magnetic anomalies on Mars. *Meteoritics & Planetary Science* 35:895–899.

Kletetschka G., Kohout T., and Wasilewski P. J. 2003. Magnetic remanence in the Murchison meteorite. *Meteoritics & Planetary Science* 35:895–899.

Kontny A., de Wall H., Sharp T. G., and Posfai M. 2000. Mineralogy and magnetic behavior of pyrrhotite from a 260 °C section at the KTB drilling site, Germany. *American Mineralogist* 85:1416–1427.

Langlais B., Purucker M. E., and Mandea M. 2004. The crustal magnetic field of Mars. *Journal of Geophysical Research* 109, doi:10.1029/2003JE002048.

Lorand J. P, Chevrier V., and Sautter V. Forthcoming. Sulfide mineralogy and redox conditions in some basaltic shergottites. *Meteoritics & Planetary Science*.

McClelland E. 1996. Theory of CRM acquired by grain growth, and its implications for TRM discrimination and palaeointensity determination in igneous rocks. *Geophysical Journal International* 126:271–280.

McEnroe S. A., Harrison R. J., Robinson P., and Langenhorst F. 2002. Nanoscale haematite-ilmenite lamellae in massive ilmenite rock: An example of 'lamellar magnetism' with implications for planetary magnetic anomalies. *Geophysical Journal International* 151:890–912.

McSween H. Y., Jr. 2002. The rocks of Mars, from far and near. *Meteoritics & Planetary Science* 37:7–25.

McSween H. Y., Jr. and Treiman A. H. 1998. Martian meteorites. In *Planetary materials*, edited by Papike J. J. Washington, D. C.: Mineralogical Society of America. pp. 6-01–6-40.

Morimoto C., Otofuji Y., Miki M., Tanaka H., and Itaya T. 1997. Preliminary paleomagnetic results of an Archean dolerite dyke of west Greenland: Geomagnetic field intensity at 2.8 Ga. *Geophysical Journal International* 128:585–593.

Nimmo F. and Gilmore M. S. 2001. Constraints on the depth of magnetized crust on Mars from impact craters. *Journal of Geophysical Research* 106:12,315–12,324.

O'Neill H. St. C. and Mavrogénes J. A. 2002. The sulfide capacity and the sulfur content at sulfide saturation of silicate melts at 1400 °C and 1 bar. *Journal of Petrology* 43:1049–1087.

Parker R. 2003. Ideal bodies for Mars magnetics. *Journal of Geophysical Research* 108, doi:1029/2001JE001760.

Peters C. and Thompson R. 1998. Magnetic identification of selected natural iron oxides and sulfides. *Journal of Magnetism and Magnetic Materials* 183:365–374.

Roberts A. P., Pike C. R., and Verosub K. L. 2000. First-order reversal curve diagrams: A new tool for characterizing the magnetic properties of natural *samples. Journal of Geophysical Research* 105:28,461–28,475.

Rochette P., Fillion G., Mattéi J. L., and Dekkers M. 1990. Magnetic transition at 30–34 K in pyrrhotite: Insight into a widespread occurrence of pyrrhotite in rocks. *Earth and Planetary Science Letters* 98:319–328.

Rochette P., Lorand J. P., Fillion G., and Sautter V. 2001. Pyrrhotite and the remanent magnetization of SNC meteorites: A changing perspective on Martian magnetism. *Earth and Planetary Science Letters* 190:1–12.

Rochette P., Fillion G., Ballou R., Brunet F., Oulladiaf B., and Hood L. 2003. High pressure magnetic transition in pyrrhotite and impact demagnetization on Mars. *Geophysical Research Letters* 30, doi:10.1029/2003GL017359.

Sautter V., Barrat J. A., Jambon A., Lorand J. P., Gillet P., Javoy M., Joron J. L., and Lesourd M. 2002. A new martian meteorite from Morocco: The nakhlite Northwest Africa 817. *Earth and Planetary Science Letters* 195:223–238.

Scott E. R. D. and Fuller M. 2004. A possible source for the Martian crustal magnetic field. *Earth and Planetary Science Letters* 220: 83–90.

Shaw J., Hill M. J., and Openshaw S. J. 2001. Investigating the ancient Martian magnetic field using microwaves. *Earth and Planetary Science Letters* 190:103–109.

Shi H. and Tarling D. H. 1999. The origin of bore-core remanences: Mechanical-shock-imposed irreversible magnetizations. *Geophysical Journal International* 137:831–838.

Terho M., Pesonen L. J., and Kukkonen I. T. 1991. The petrophysical classification of meteorites: New results. Geological Survey of Finland Q29.1/91/1. Espoo, Finland. 95 p.

Weiss B. P., Vali H., Baudenbacher F. J., Kirschvink J. L., Stewart S. T., and Shuster D. L. 2002. Records of an ancient Martian magnetic field in ALH 84001. *Earth and Planetary Science Letters* 201:449–463.

Weiss B. P., Kim S. S., Kirschvink J. L., Kopp R. E., Sankaran M., Kobayashi A., and Komeili A. 2004. Magnetic tests for magnetosome chains in Martian meteorite ALH 84001, *Proceedings of the National Academy of Sciences* 101:8281–8284.

Wehland F., Stancu A., Rochette P., Dekkers M., and Appel E. Forthcoming. Experimental determination of magnetic interaction in natural and artificial pyrrhotite bearing samples. *Geophysical Journal International*.

Xirouchakis D., Draper D. S., Swhandt C. S., and Lanzirotti A. 2002. Crystallization conditions of Los Angeles, a basaltic Martian meteorite. *Geochimica et Cosmochimica Acta* 66:1867–1880.

Yu Y. J., Dunlop D. J., Özdemir Ö., Ueno H. 2001. Magnetic properties of Kurokami pumices from Mt. Sakurajima, Japan. *Earth and Planetary Science Letters* 192:439–446.